UCRL-84534
PREPRINT

TWO-DIMENSIONAL SLOPE WIND SIMULTIONS IN THE FINITE ELEMENT APPROXIMATION

Dieter R. Tuerpe

THIS PAPER WAS PREPARED FOR
SUBMITTAL TO THE ASCOT PROGRAM
PLANNING MEETING, GETTYSBURG, PA
APRIL 15-18, 1980.

June 1980

UCRL-84534

TWO-DIMENSIONAL SLOPE WIND SIMULATIONS IN THE FINITE ELEMENT APPROXIMATION*

Dieter R. Tuerpe

Lawrence Livermore National Laboratory, University of California
Livermore, California 94550

June 1980

ABSTRACT

The hydrostatic fluid dynamics model developed at LLL has been used to simulate the development of katabatic winds. This model solves the Navier-Stokes equations in the Boussinesq approximation by the finite element method. Preliminary results indicate that to obtain physically reasonable results one has to choose unequal diffusion parameters in the horizontal (K_x) and vertical (K_z). The maximum velocities obtained with K_z = 1 m^2/sec and K_x = 100 m^2/sec are of the order of 2.5 m/sec for a slope of .2. Profiles of the downslope velocities will be presented at different points in the flow. As expected, the magnitude of the vertical diffusion coefficient K_z controls the depth of the flow which seems to increase only slightly with downhill distance, and the magnitude of the flow increases with cooling rate and slope.

*This work was performed under the auspices of the U. S. Department of Energy by the Lawrence Livermore National Laboratory under contract No. W-7405-Eng-48.

TWO-DIMENSIONAL SLOPE WIND SIMULATIONS IN THE FINITE ELEMENT APPROXIMATION

A. Introduction

Slope winds, i.e., winds produced by the sustained cooling of a slope at night seem to be the most important ventilation mechanism in complex terrain in the absence of strong synoptic pressure gradients, and thus become important for air quality models in complex terrain.

The historical development of slope winds modeling and observation are treated in Thyer (1966) and more recently in Manins and Sawford (1979a). The first model of slope winds was proposed by Prandtl (1942, see Sutton 1953) and was limited by the assumption that the winds were steady along the slope, thus reducing the problem to one dimension. Another approach is to consider only an average flow within the cooled layer, eliminating all internal structure of the wind field (Petkovsek and Hocevar, 1971). This approach has been generalized by Manins and Sawford who impose three profile factors on the flow, thus the vertical structure of the katabatic wind field is determined a priori and the subsequent time development of the flow is dependent on the initial guess of these profile factors.

The third approach to the modeling of drainage is the numerical solution of a set of primitive equations for the atmosphere. This was first done by Thyer (1966), L. M. Leslie and K. R. Smith (1974) and more recently by C. P. Stevens (1979). The latter calculation was only done for one set of parameters, i.e., one slope and one cooling rate and with closed boundaries. Yamada (1980) has applied his second order closure model to the problem of slope winds.

In the following, I will present results for a primitive equation model (Navier-Stokes equations in the Boussinesq approximation) solved by a finite element numerical algorithm. In Section B I will present a short summary of the equations. The results are discussed in Section C where the emphasis has been on a variation of the key parameters: diffusivity, slope and cooling rates. Finally, the conclusions drawn from these runs and the feasibility of an extension of the model to three dimensions will be discussed in Section D.

B. Model Equations

The model used was the LLL hydrostatic fluid dynamics model developed by Chan et al.(1979). This model uses the Navier-Stokes equations in the Boussinesq approximation i.e., in two dimensions

$$\rho \left(\frac{\partial u}{\partial t} + u \frac{\partial u}{\partial x} + w \frac{\partial u}{\partial z}\right) = - \frac{\partial p}{\partial x} + K_x \frac{\partial u^2}{\partial x^2} + K_y \frac{\partial u^2}{\partial y^2} \tag{1}$$

$$\frac{\partial p}{\partial y} = \rho g \gamma T \tag{2}$$

$$\frac{\partial u}{\partial x} + \frac{\partial w}{\partial z} = 0 \tag{3}$$

$$\frac{\partial T}{\partial t} + u \frac{\partial T}{\partial x} + w \frac{\partial T}{\partial z} = K_x^T \frac{\partial^2 T}{\partial x^2} + K_z^T \frac{\partial^2 T}{\partial z^2} \tag{4}$$

Where u is the horizontal velocity, w is the vertical velocity, p the pressure deviation from equilibrium, T is the temperature deviation from equilibrium, ρ is the density, g the acceleration of gravity, γ the coefficient of thermal expansion K_x, K_z, K_x^T and K_z^T are the momentum and temperature diffusion coefficients respectively.

To solve this system of equations in the finite element method, one expands the unknowns, u, w, p, and T in the equation in highly localized polynomials and solves for the expansion coefficients, i.e.

$$\begin{aligned} u &= \Sigma_i \, u_i \, \phi_i \, (x,z) \\ w &= \Sigma_i \, w_i \, \phi_i \, (x,z) \\ T &= \Sigma_i \, T_i \, \phi_i \, (x,z) \\ p &= \Sigma_i \, p_i \, \psi_i \, (x,z) \end{aligned} \tag{5}$$

These expansions are then substituted into the original equations and after applying some weighted residual method (in this case, Galerkin for equations (1) and (4), least squares for equations (2) and (3)), one obtains a set of algebraic equations which may be solved for the expansion coefficients. For a much more complete discussion of the numerical methods employed, the reader is referred to Chan (1979).

The choice of the hydrostatic code for these calculations deserves some discussion. The non-hydrostatic FEM code has at the moment the fundamental limitation of requiring the pressure basis functions to be polynomials of one order lower than the basis functions for the velocity, and temperature. This means in practice that the pressure basis functions are restricted to be either piecewise constant or piecewise linear polynomials. On the other hand, a linear temperature distribution, the simplest non-trivial temperature deviation from equilibrium, will induce a quadratic pressure variation. Trying to represent this quadratic pressure fluctuation with either linear or

piecewise constant pressure basis functions leads to a large error in the pressure gradient across the grid in the presence of topography (Tuerpe, 1980). The hydrostatic fluid dynamics code has the capability of quadratic pressure basis functions and has been used in the obtaining the results of the next section.

C. Results

Most of the runs, with the exception of those with a different slope, were made with the grid of Fig. 1, which has 341 node points, 11 in the vertical and 31 in the horizontal. The basis functions for all variables are quadratic, defined on the standard 9-node element. The boundary conditions are as indicated in Fig. 1, with open top and lateral boundary, and a no flow bottom boundary. The bottom boundary was then cooled uniformly according

to $T_G = C_1 \sin \frac{t}{C_2}$

Where T_G = ground temperature,

and t = time.

Fig. 2 shows the vector field of a typical run after about 2 hrs. A drainage layer about 100 meters high is formed above the ground and the air starts flowing down the mountain with a velocity of about 2-3 m/sec. In all of these runs the momentum diffusivities are assumed to be equal to the temperature diffusivities.

Figs. 3, 4 and 5 show the profiles of the velocity along the slope at different points on the slope. It is seen that in all three cases the depth of the drainage layer increases slightly with distance along the slope and that this depth is controlled by the magnitude of K_z, i.e., the larger K_z, the larger the drainage layer. Fig. 6 shows the maximum velocity within the drainage layer as a function of slope. As expected, for the same rate of cooling of the ground, the larger the slope, the larger the drainage velocity. Fig. 7 shows the maximum velocity along the slope as a function of the vertical diffusivity. The falloff in the magnitude of the velocity near the bottom of the slope occurs because the drainage layer abruptly widens due to the change in slope at the bottom and this effect is more pronounced for a wider initial drainage layer, i.e., a run with a higher K_z. Fig. 8 shows the maximum velocity as a function of various parameters. Curve 2 has the same parameters as curve 1, except plotted at a later time. Since equilibrium has not yet been reached, the downslope velocity is still increasing, as expected. Curve 3 on Fig. 8 is the same as curve 1 except with the cooling rate doubled.

Finally, Fig. 9 shows an attempt to model upslope flow. In this run the surface is heated, as occurs early in the morning when the sun first begins to shine on the slope. This situation is much more unstable than that in which the slope was cooled. Here cool air is above warm air and the slope changes induce instability into the flow which produce large vertical velocities. It is not quite clear whether these large vertical velocities in the model run come about because of the nature of the hydrostatic approximation, which breaks down at points of high vertical acceleration, or whether they are a realistic consequence of the physics of this highly unstable situation.

D. Conclusions

The results reported in this paper have demonstrated that the finite element approximation is useful for solutions of the Navier-Stokes equations with atmospheric applications, provided one has chosen quadratic or higher order polynomials as the pressure basis functions when atmospheric process over complex terrain are modeled. Detailed comparison of these two-dimensional results to experiment, other than very qualitative observations, are not appropriate, since two-dimensional slopes do not usually occur in nature. However, the orders of magnitude of the velocity (2-4 m/sec) compares well with the results of the 1979 ASCOT Geysers experiment and the measurements of Manins and Sawford (1979b). The vertical profile of the drainage velocity is very similar to that measured by Manins and Sawford, but differs with the 1979 Geysers data where the profile is much broader than in the present calculations. This might be due to a canopy drag factor, neglected in the present model. Yamada (1980) appears to obtain broader profiles when such a canopy drag factor is included. In addition, the terrain in the Geysers is very complex, while the site for the Manins and Sawford experiment was close to an idealized two-dimensional slope.

The calculations reported here were done as an intermediate step to the development of a three-dimensional atmospheric dynamics code valid in complex terrain. One should also investigate the validity of the hydrostatic approximation for slope winds. Here the requirement of a quadratic pressure basis function in the finite element approximation causes some difficulty, since the velocity and temperature basis functions should be one order higher than the pressure basis functions for a nonhydrostatic formulation. This would mean that the basis functions for the velocity and temperature would have to be cubic, however, mesh generators for grids appropriate to cubic basis functions do not exist. One approach to overcome this would be to construct an "almost" nonhydrostatic code by reinserting the vertical acceleration terms but not the diffusion terms into the hydrostatic formulation. This procedure also allows one to retain the simple boundary conditions of the hydrostatic code. Another approach would simply be to ignore the bad pressure solution obtained with a nonhydrostatic fluid dynamics code where the pressure and velocity basis functions are of the same order. Here the spurious part of the pressure solution does not act as a driving term for the velocity.

Both the development of the 3-D hydrostatic fluid dynamics code and the reformulation of the nonhydrostatic code as a check on the validity of the hydrostatic approximation are being implemented at LLL.

Acknowledgments

I thank Drs. Philip Gresho, Robert Lee, and Marvin Dickerson for many useful discussions of this problem. Special thanks go to Dr. Stevens Chan, who graciously made his code available to me and was always ready to discuss the results.

Figure Captions

Figure 1. The grid used in the model runs for a slope of .2. Boundary conditions are indicated on the figure.

Figure 2. A typical vector flow-field at t = 6800 sec, $K_x = K_x^T$ = 100 m^2/sec, $K_z = K_z{}^T$ = 1 m^2/sec, T_G = -20 sin t/27000, slope = .2.

Figure 3. Profile of the velocity along the slope, same parameters as figure 2 except for $K_z^T = K_z$ = .1 m^2/sec and t = 4153 sec.

Figure 4. Profile of the velocity along the slope, same parameters as Fig. 3 except $K_z = K_z^T$ = 1.0 m^2/sec.

Figure 5. Profile of velocity along the slope, same parameters as Fig. 3 except $K_z = K_z^T$ = 5.0 m^2/sec.

Figure 6. Maximum velocity along the slope as a function of K_z
T_G = -20 sin t/27000, t = 4100 sec, $K_x = K_x^T$ = 100 m^2/sec, slope = .2

Curve 1: $K_z = K_z^T$ = .1 m^2/sec

Curve 2: $K_z = K_z^T$ = 1.0 m^2/sec

Curve 3: $K_z = K_z^T$ = 5.0 m^2/sec

Figure 7. Maximum velocity along the slope as a function of slope.
T_G = -20 sin t/27000, t = 4100 sec, $K_x = K_x^T$ = 100 m^2/sec
$K_z = K_z^T$ = 1.0

Curve 1: Slope = .1
Curve 2: Slope = .2
Curve 3: Slope = .3

Figure 8. Maximum velocity along the slope as a function of time and cooling rate.
$K_x = K_x^T$ = 100 m^2/sec, $K_z = K_z^T$ = 1 m^2/sec, slope = .2

Curve 1: T_G = -20 sin t/2700, t = 4058 sec
Curve 2: T_G = -20 sin t/2700, t = 6800 sec
Curve 3: T_G = -40 sin t/2700, t = 4092 sec.

Figure 9. Upslope wind after 2700 sec. T_G = 20 sin t/2700, K_x = K_x^T = 100 m^2/sec, $K_z = K_z^T$ = 1 m^2/sec.

References

Chan, S. T., P. M. Gresho and R. L. Lee, 1979: Simulation of LNG vapor spread and dispersion by finite element methods. Presented at National Conf. on Num. Methods in Heat Transfer, Univ. of Maryland, Sept. 24-26, 1979. UCRL-82441.

Leslie, L. M. and K. R. Smith, 1974: A numerical simulation of katabatic winds and their effect on pollutant dispersal in urban areas. Proc. 5th Australasian Conf. Hydraulic Fluid Mechanics, Univ. of Cantaberra, Christ Church N.Z., D. Lindley and A. Sutherland, Eds., Vol. 2, 553-560.

Manins, P. C. and Sawford, 1979a: A model of katabatic winds. J. Atmos. Sci. 36, 619-630.

Manins, P. C. and B. L. Sawford, 1979b: Katabatic winds: a field case study. Quart. J. R. Met. Soc. 105, 1011-1025.

Petkovsek, A. and A. Hocevar, 1971: Night drainage winds. Arch. Meteor. Geophys. Bioklim A20, 353-360.

Stevens, C. P., 1978: Finite element solution for a fluid subject to thermal and buoyancy effects in numerical simulation of fluid motion, ed. John Noye, 551-566, North Holland Publishing Co. (1978).

Sutton, O. G., 1953: Micrometeorology, McGraw Hill.

Thyer, N. H., 1966: A theoretical explanation of valley and mountain winds by a numerical method. Arch. Meteor. Geophys. Bioklim. A15, 318-348.

Tuerpe, D. R., 1980, to be published.

Yamada, T., 1980, private communication.

DRT:clm:1227z

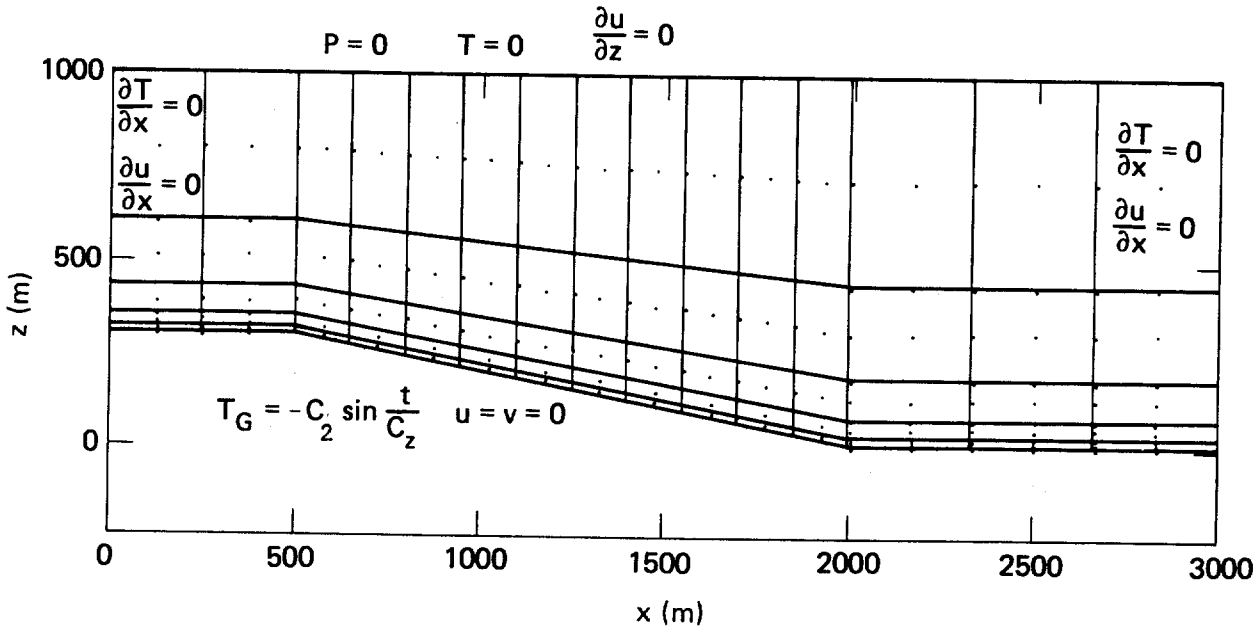
P = 0
T = 0
∂u/∂z = 0
∂T/∂x = 0
∂u/∂x = 0
∂T/∂x = 0
∂u/∂x = 0
T_G = -C_2 sin t/C_z
u = v = 0
1000
500
0
z (m)
0
500
1000
1500
2000
2500
3000
x (m)

Figure 1.

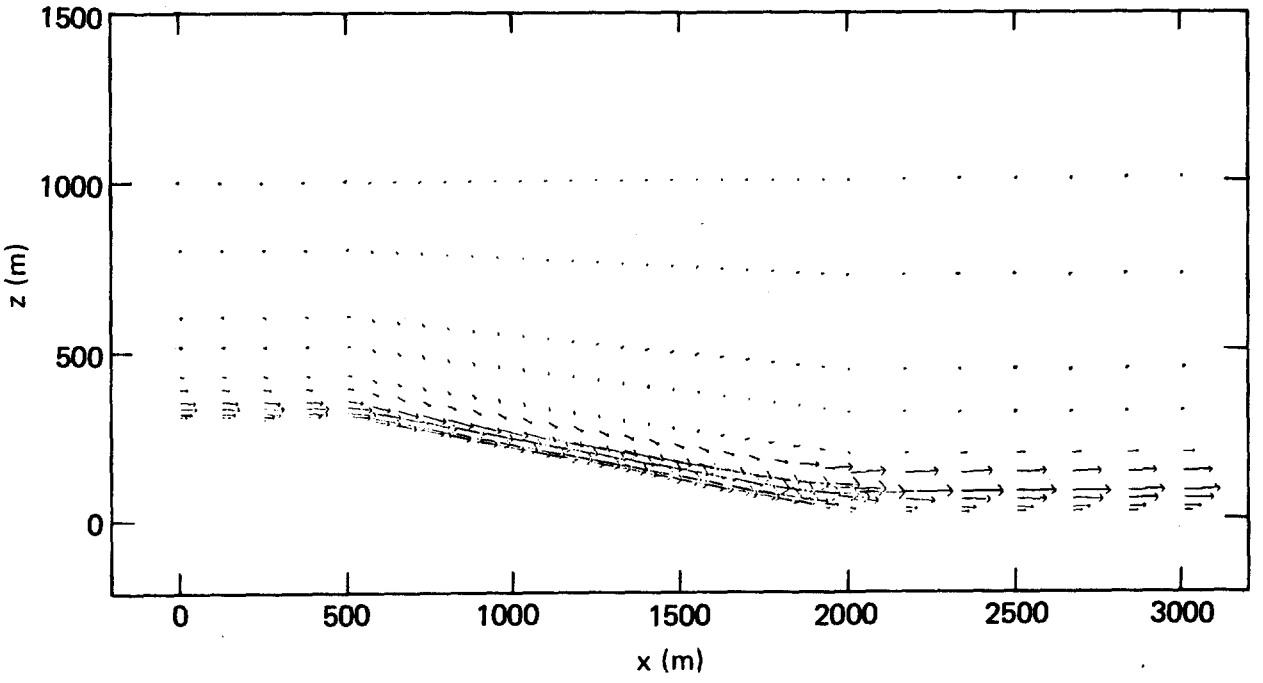

Figure 2.

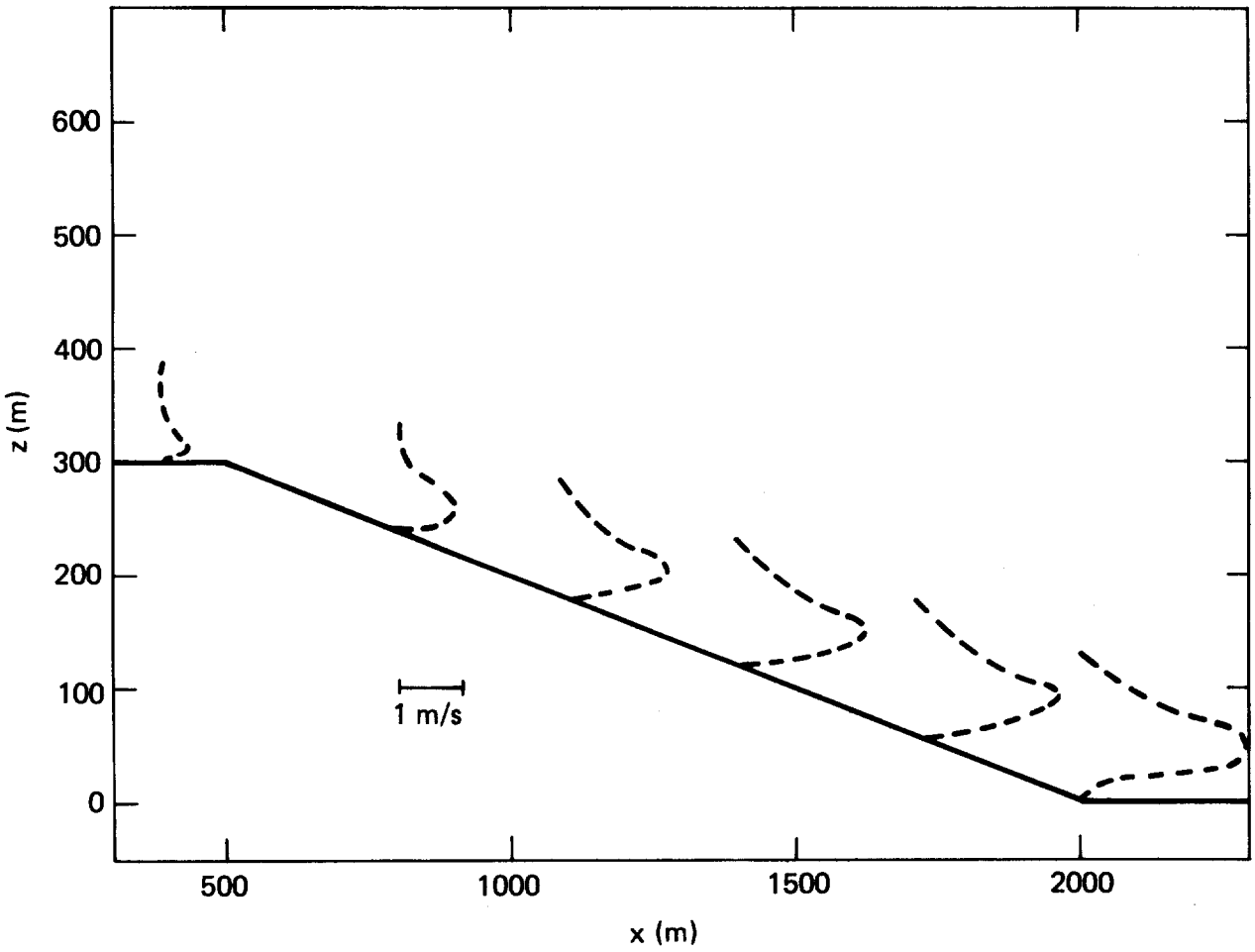

Figure 3.

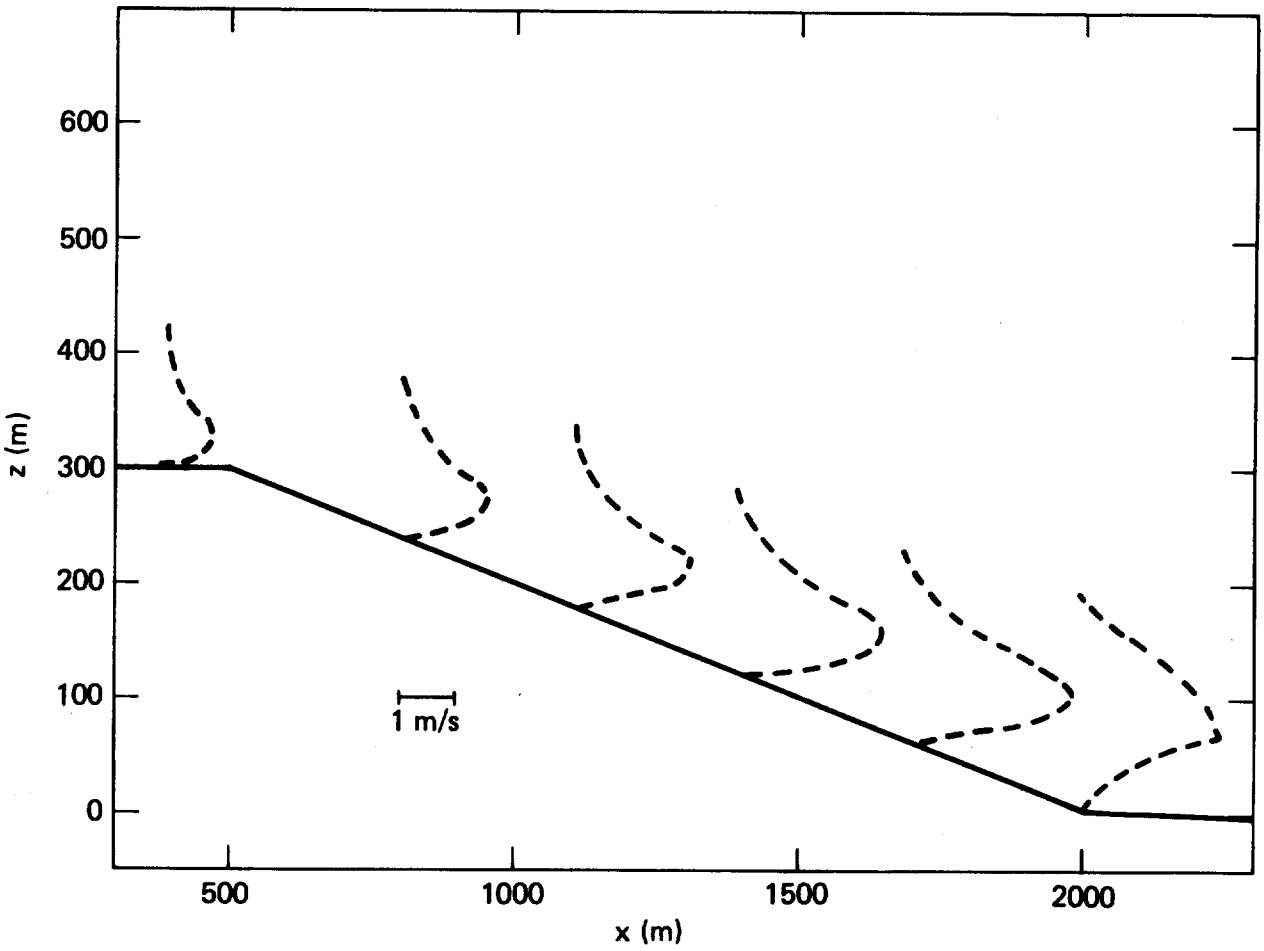

Figure 4.

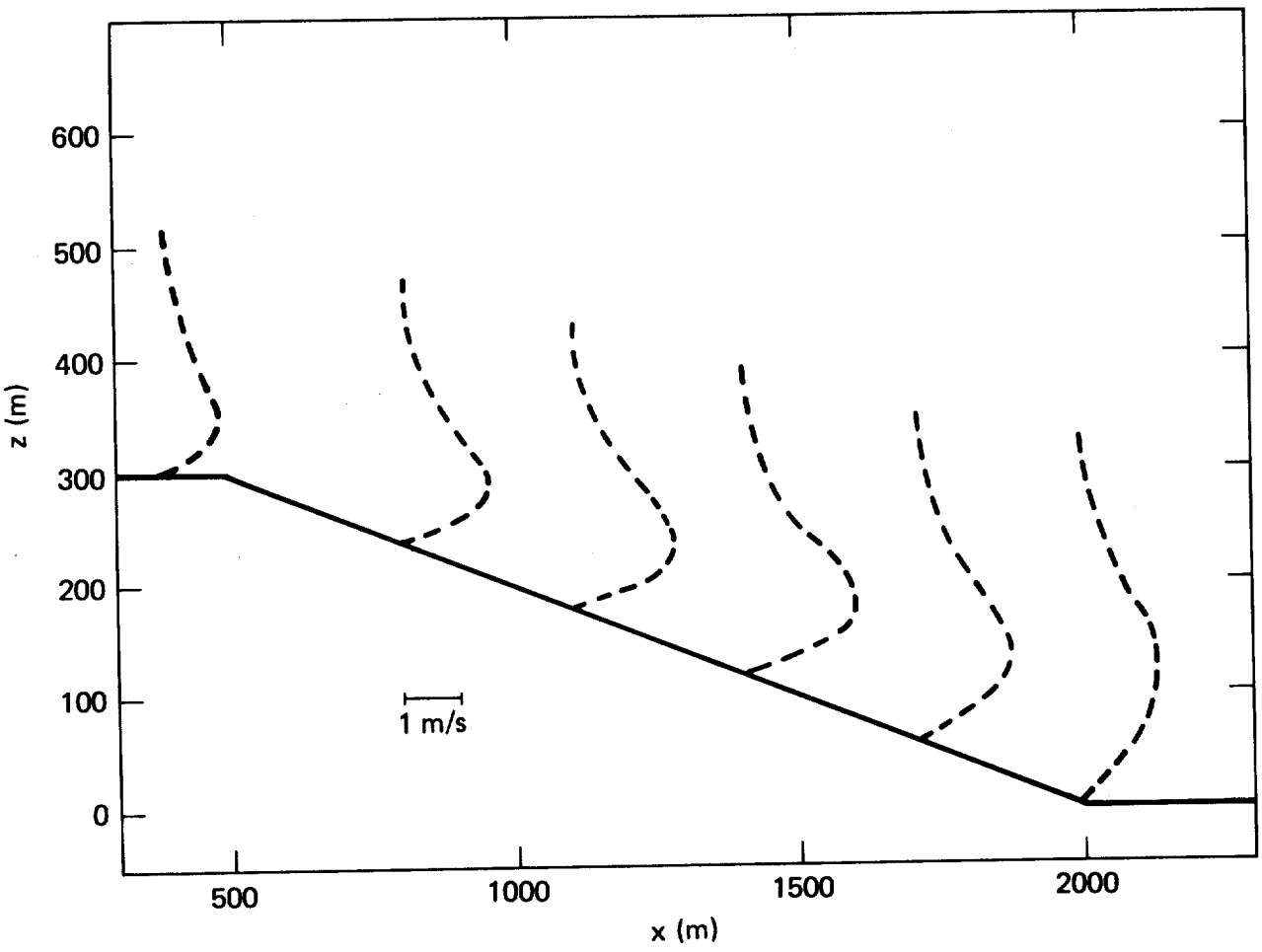

Figure 5.

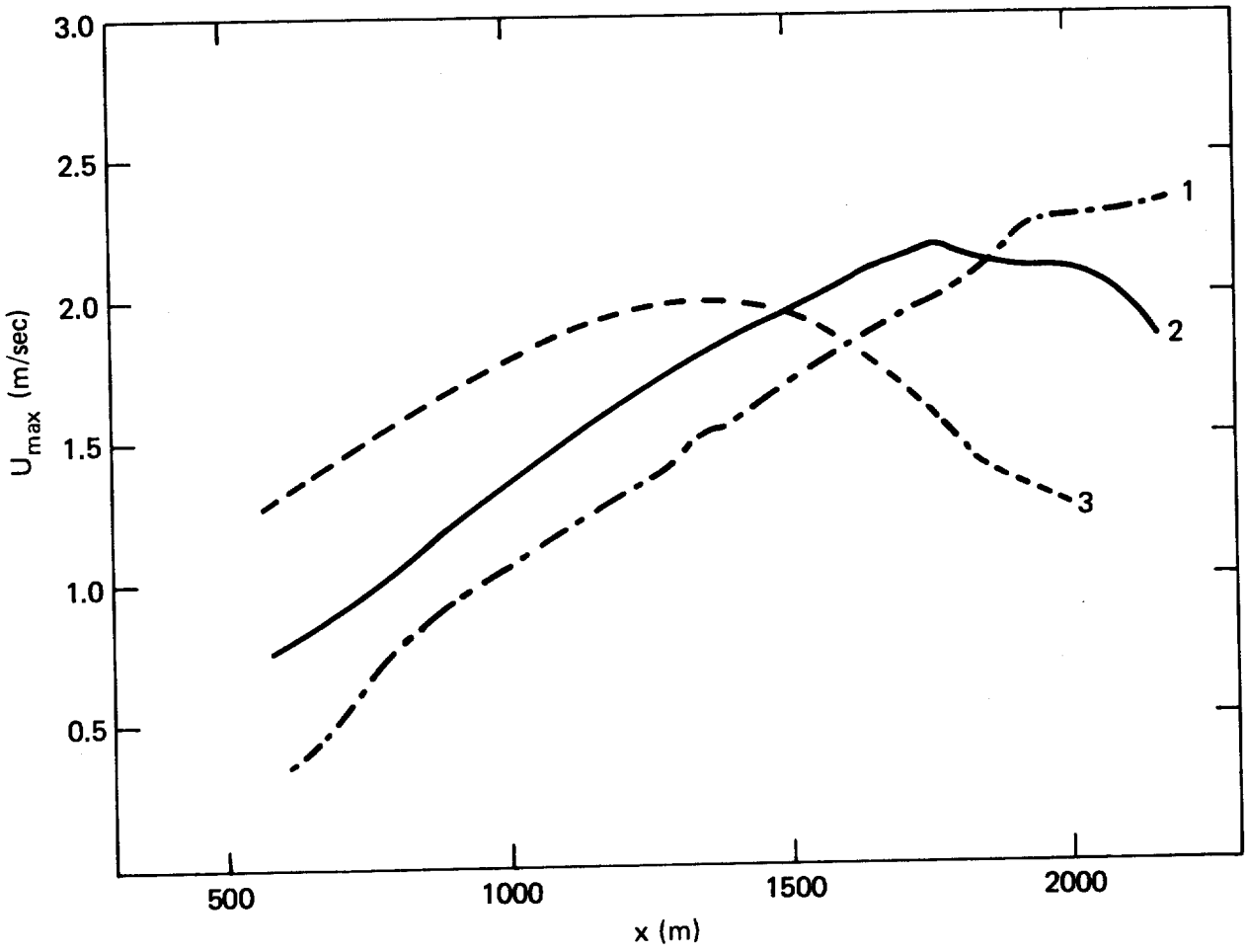

Figure 6.

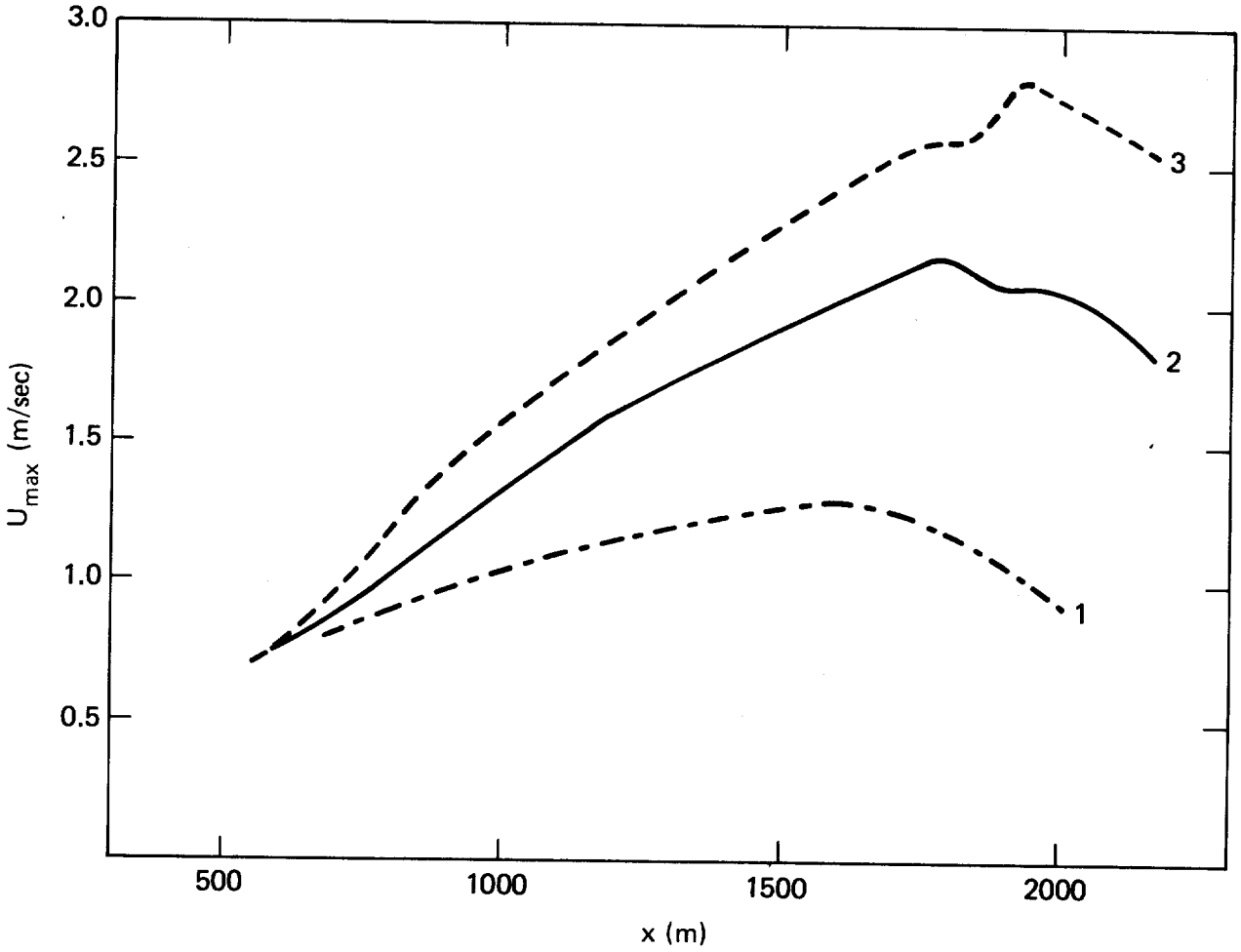

Figure 7.

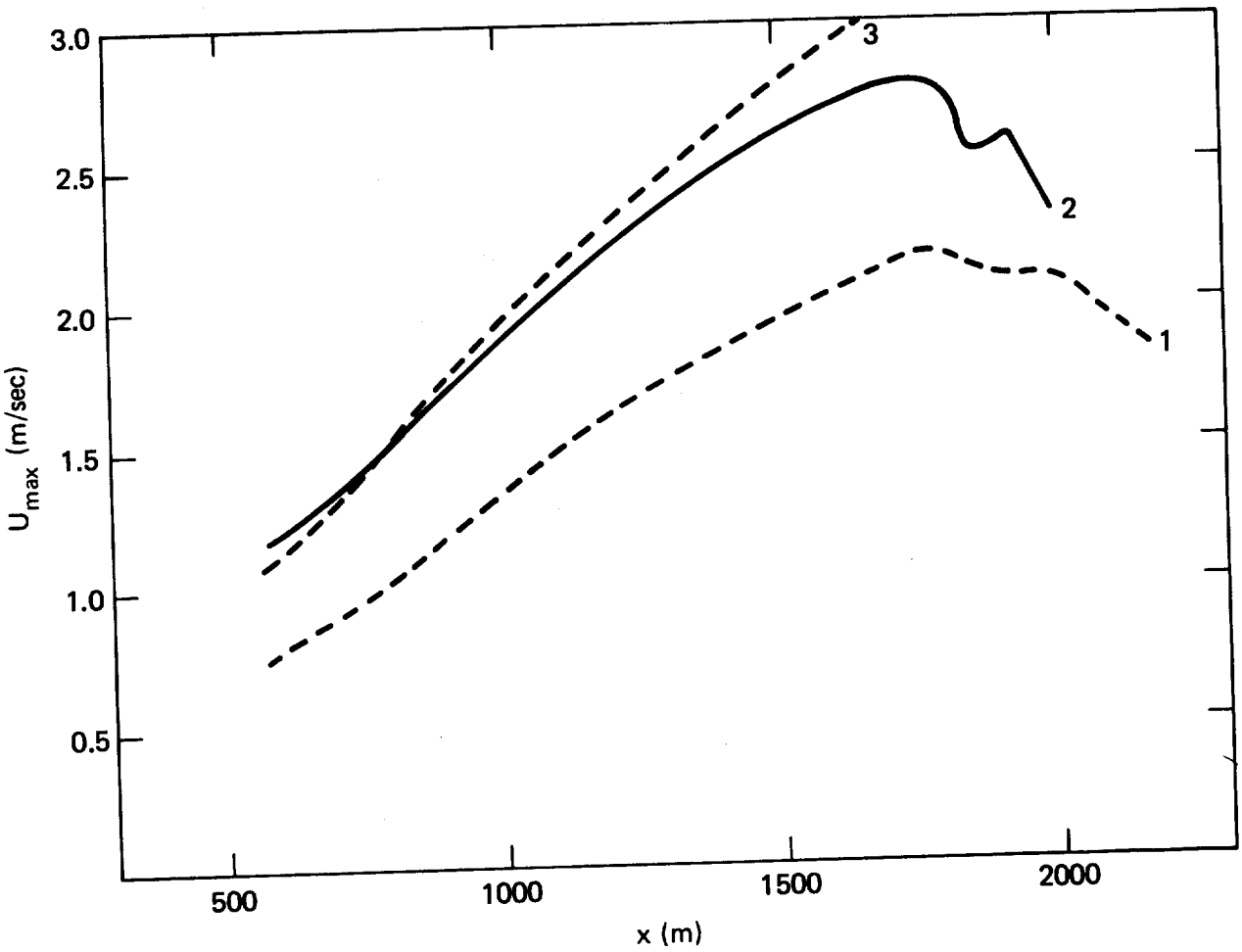

Figure 8.

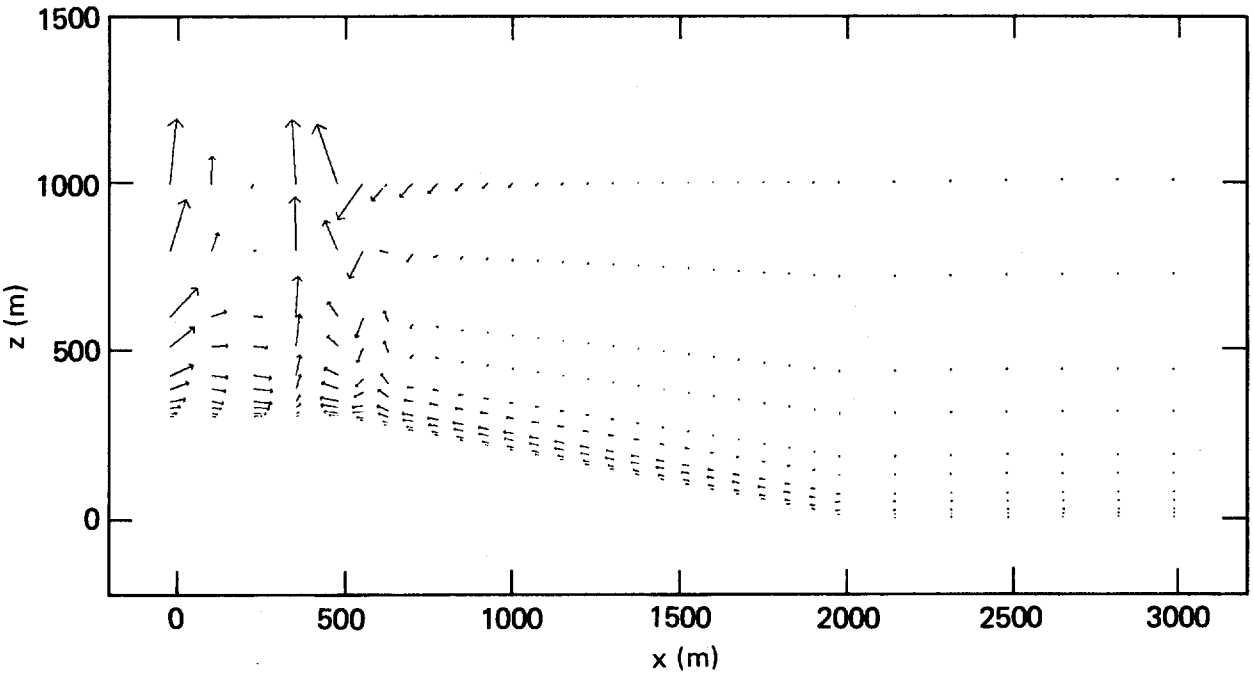

Figure 9.